Spectroscopic, electrochemical and computational study of Pt-diimine-dithiolene complexes: Rationalising the properties of solar cell dyes

Post-print of a peer-reviewed article published by the Royal Society of Chemistry.
Published article available at: http://dx.doi.org/10.1039/B719789F

Cite as:
Geary, E. A. M., McCall, K. L., Turner, A., Murray, P. R., McInnes, E. J. L., Jack, L. A., Yellowleesa, L. J., & Robertson, N. (2008). Spectroscopic, electrochemical and computational study of Pt-diimine-dithiolene complexes: Rationalising the properties of solar cell dyes. *Dalton Transactions*, (28), 3701-3708.

Manuscript received: 02/01/2008; Accepted: 22/04/2008; Article published: 29/05/2008

Spectroscopic, Electrochemical and Computational Study of Pt-diimine-dithiolene Complexes: Rationalising the Properties of Solar Cell Dyes**

Elaine A. M. Geary,[1] Keri L. McCall,[1] Andrew Turner,[1] Paul R. Murray,[1] Eric J. L. McInnes,[2] Lorna A. Jack,[1] Lesley J. Yellowlees[1] and Neil Robertson[1,*]

[1]EaStCHEM, School of Chemistry, Joseph Black Building, University of Edinburgh, West Mains Road, Edinburgh, EH9 3JJ, UK.

[2]School of Chemistry, University of Manchester, Oxford Road, Manchester, UK.

[*]Corresponding author; e-mail: neil.robertson@ed.ac.uk; fax: +44 1316504743 ; tel: +44 1316504755

[**]We thank the University of Edinburgh Christina Miller fund and the EPSRC Excitonic Solar Cells Supergen Consortium for financial support and we thank the EPRSC Multifrequency EPR National Service.

Supporting information:
[†]Electronic supplementary information (ESI) available: Table S1: UV/Vis of oxidised and reduced species; Fig. S1–S4: UV/Vis spectra of **2a**$^{0/1-}$, **2b**$^{0/1-/2-}$, **2c**$^{0/1-/2-}$, **2c**$^{0/1+}$; Fig. S5–S7: EPR of**1b**$^{1-}$, **2c**$^{1-}$, **1b**$^{1-}$ (frozen); Tables S2 and S3: frontier orbital energies of **2a**, **3a**; Table S4: calculated contribution of ring C and N atoms to the LUMO of **1c**, **2c**, **3c**; Table S5: calculated frontier orbital energies of **1b**, **1c**, **2c**, **3c**; Fig. S8–S17 representations of frontier orbitals of **2a**, **3a**, **2c**, **3c**, **1b**; Table S6: comparison of calculated and experimental structure of **1c**; Table S7: calculated energies and % contributions of HOMO and LUMO for **1b**, **1c**, **2c**, and **3c**; Tables S8–S10: TD-DFT results for **1c**, **2c**, **3c**; Fig. S10: TD-DFT results for **2c**, **3c**. See http://dx.doi.org/10.1039/B719789F

Abstract

A series of [Pt(II)(diimine)(dithiolate)] complexes of general formula [Pt{X,X′$(CO_2R)_2$-bpy}(mnt)] (where X= 3, 4 or 5; R= H or Et, bpy = 2,2′-bipyridyl and mnt = maleonitriledithiolate), have been spectroscopically, electrochemically and computationally characterised and compared with the precursors [Pt{X,X′-$(CO_2R)_2$-bpy}Cl_2] and X,X′$(CO_2R)_2$-bpy. The study includes cyclic voltammetry, *in-situ* EPR spectroelectrochemical studies of fluid solution and frozen solution samples, UV/Vis/NIR spectroelectrochemistry, hyrid DFT and TDDFT calculations. The effect of changing the position of the bpy substituents from 3,3′ to 4,4′ and 5,5′ is discussed with reference to electronic changes seen within the different members of the family of molecules. The performance of the mnt complexes in dye-sensitised solar cells has been previously described and the superior performance of [Pt{3,3′-$(CO_2R)_2$-bpy}(mnt)] is now explained in terms of decreased electronic delocalisation through twisting of the bipyridyl ligand as supported by the EPR and computational results.

Introduction

Complexes of Pt(II) with polypyridyl ligands have been widely studied due to properties including redox activity, solvatochromism and luminescence.[1, 2] In most cases, ligands on the Pt centre can be readily varied, allowing for manipulation of the molecular and electronic properties of these complexes making them useful as model systems for the study of many physical properties. In recent years square-planar Pt(II) coordination complexes have also been studied for their potential use in the area of Dye-Sensitised Solar Cells (DSSC)[3-6] and in solar to chemical energy conversion.[7] In a DSSC, a dye molecule is adsorbed on to the surface of a semiconductor (usually TiO_2). Upon illumination with visible light, the photo-excited dye injects an electron into the conduction band of the semiconductor, which is supported on a transparent electrode. The dye is re-reduced by a redox couple (typically I^-/I_3^-), which in turn is regenerated at the counter electrode, thus completing the circuit.[8]

The dye molecule in a DSSC requires a linker moiety which attaches the dye to the surface of the semiconductor[9] and in the large majority of studies this has been the (4,4′-$CO_2H)_2$-bpy ligand (bpy = 2,2′-bipyridyl). The 4,4′-substituted carboxylic acid groups on the bpy bind to the surface of the semiconductor allowing electron transfer from the excited dye molecule to the semiconductor. This electron transfer reaction is facilitated by the interaction of the π^* orbital on the substituted bpy with the 3d orbital manifold of the conduction band of the TiO_2.

An attractive feature of [Pt(diimine)(dithiolene)] complexes is the ease with which the HOMO and LUMO of the molecule can be separately tuned. Over the past two decades, Eisenberg *et al.* have systematically studied the electrochemistry and luminescence of a range of these molecules by sequentially changing the substituents on the diimine and dithiolene components.[2] This has shown that the excited state energies can be tuned by up

to 1 eV. Such studies have demonstrated that the LUMO on [Pt(II)(diimine)(dithiolate)] complexes is located on the diimine functionality and the HOMO is a mixture of Pt(d) and S(p) orbital character. The visible charge-transfer transition for these molecules is therefore assigned as a MMLL′CT (Mixed Metal-Ligand to Ligand Charge Transfer) from the Pt/S HOMO to the diimine based LUMO.[1,2,10] These previous studies have focussed almost exclusively on complexes with 4,4′-disubstitued diimine ligands.[1,2,10]

We have recently reported the synthesis and study in DSSC of a series of [Pt(II)(diimine)(dithiolate)] complexes, that bind to the semiconductor surface through a bpy ligand substituted with carboxylic acid groups at the positions, 3,3′, 4,4′ and 5,5′ respectively. The solar-energy conversion efficiencies of the resulting complexes were studied and interestingly showed the 3,3′-disubstituted bpy molecule to be the most efficient sensitiser of those tested.[6] In marked contrast, studies of Ru-bpy dyes (the most efficient class of sensitiser) in DSSC have focussed almost entirely on 4,4′-substitution. We are only aware of one Ru dye involving 3,3′-$(CO_2H)_2$-bpy ligands that has been studied in DSSC and this showed slightly poorer results than the analogous Ru complex with 4,4′-$(CO_2H)_2$-bpy ligands.[11] Presumably, the slightly poorer performance is the reason for the lack of further interest, however our results on Pt complexes suggest that 3,3′-$(CO_2H)_2$-bpy ligands are worth revisiting.

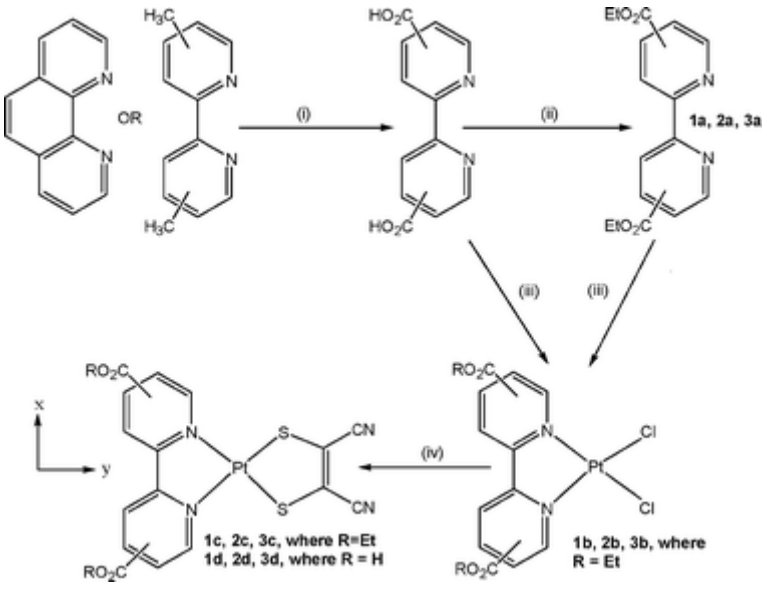

Figure 1. Synthesis of members of the family of [Pt{X,X′-$(CO_2R)_2$-bpy}(mnt)]. (i) $KMnO_{4(aq.)}$, 120°C/HCl (ii) EtOH/H_2SO_4, 115°C (iii) K_2PtCl_4, 125°C (iv) Na_2(mnt), RT (140°C for **2c**). The principle axis system for the EPR analysis is also shown with the z-axis perpendicular to the molecular plane.

Following this discovery, the aim of the current work is to greatly extend our understanding of the electronic properties of [Pt{X,X′-$(CO_2Et)_2$-bpy}(mnt)] (X = 3, 4 or 5; mnt = maleonitriledithiolate) by systematic

electronic characterision of each member of this family and comparison with related precursors, (Fig. 1) using UV/Vis/NIR spectroelectrochemistry, *in-situ* EPR spectroelectrochemistry and DFT calculations. In particular, this allows insight into the bpy based LUMO which influences not only the photophysical and electronic properties of the molecules, but also the coupling to TiO_2 and consequent electronic properties of the composite system. We have reported some initial work on the UV/Vis/NIR spectroelectrochemistry of **1c** – **3c**[6] in our original study and this is incorporated here in the discussion.

Results and Discussion

(i) Electrochemistry

The electrochemistry of the [Pt{X,X′-$(CO_2Et)_2$-bpy}(mnt)] family (**1c** – **3c**), the related [Pt{X,X′-$(CO_2Et)_2$-bpy}Cl_2] precursor molecules (**1b** – **3b**) and the corresponding uncoordinated bpy ligands (**1a – 3a**) was studied by cyclic voltammetry in solution of 0.1 M $TBABF_4$ in DMF at 293 K. Redox potentials for all processes are listed in table 1.

Table 1. Redox potentials of the [Pt{X,X′-$(CO_2Et)_2$-bpy}(mnt)] family and related precursor molecules and ligands. *irreversible, §quasi reversible reduction

No.	Compound	E_2/V	E_1/V	E_{ox}/V
1a	3,3′-$(CO_2Et)_2$-bpy	-	-1.84§	-
1b	[Pt{3,3′-$(CO_2Et)_2$-bpy}Cl_2]	-1.27	-0.61	-
1c	[Pt{3,3′-$(CO_2Et)_2$-bpy}(mnt)]	-1.20	-0.59	1.35*
1d	[Pt{3,3′-$(CO_2H)_2$-bpy}(mnt)]	-1.05*	-0.69*	1.27*
2a	4,4′-$(CO_2Et)_2$-bpy	-	-1.53	-
2b	[Pt{4,4′-$(CO_2Et)_2$-bpy}Cl_2]	-1.25	-0.67	-
2c	[Pt{4,4′-$(CO_2Et)_2$-bpy}(mnt)]	-1.20	-0.65	1.39*
2d	[Pt{4,4′-$(CO_2H)_2$-bpy}(mnt)]	-1.19§	-0.82*	1.27*
3a	5,5′-$(CO_2Et)_2$-bpy	-1.61	-1.23	-
3b	[Pt{5,5′-$(CO_2Et)_2$-bpy}Cl_2]	-1.03	-0.53	-
3c	[Pt{5,5′-$(CO_2Et)_2$-bpy}(mnt)]	-0.99	-0.52	1.41*
3d	[Pt{5,5′-$(CO_2H)_2$-bpy}(mnt)]	-1.16§	-0.69*	1.27*

The electrochemical properties show various trends which are common within each of the 3,3′, 4,4′ and 5,5′ motifs. In each case the free bpy ligand shows either one or two reductions within the solvent window. On binding to the Pt centre, the reduction potentials significantly shift to more positive values due to the stabilisation of the LUMO after complexation of the free ligand to the Pt metal. On substitution of the two chloride ligands with the mnt ligand, each [Pt{X,X′-$(CO_2Et)_2$-bpy}(mnt)] complex (**1c**, **2c** and **3c**) shows two fully reversible reductions, the potentials of which remain similar to those of their respective [Pt{X,X′-

$(CO_2Et)_2$-bpy}Cl_2] precursors (Fig. 2), particularly for the first reduction. This shows that there is only a small effect on the LUMO of the complex after substitution of the chloride ligands for mnt, consistent with assignment of the LUMO as bpy based.[2]

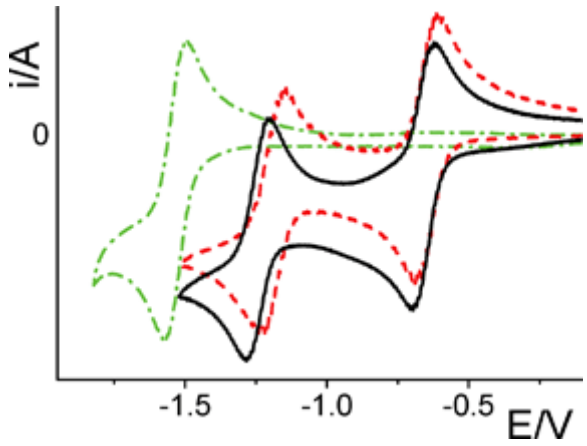

Figure 2. Cyclic voltammogram showing reduction processes for **2a** (dash-dot green), **2b** (solid black) and **2c** (dashed red) in 0.1 M TBABF4/DMF at 293K and scan rate 0.1 V/s.

In addition, each of the [Pt{X,X′-$(CO_2Et)_2$-bpy}(mnt)] complexes (**1c**, **2c** and **3c**) shows one irreversible oxidation at similar potential to each other, consistent with location of the HOMO on the dithiolate moiety.

Reduction of the free ligand becomes harder in the order {5,5′-$(CO_2Et)_2$-bpy}, {4,4′-$(CO_2Et)_2$-bpy}, {3,3′-$(CO_2Et)_2$-bpy}, since the electron-withdrawing groups at the 5,5′ position of the bpy provide greater stabilisation of the monoanion than substituents at the 4,4′ or 3,3′ positions.[12] The electrochemistry of [Pt{5,5′-$(CO_2Et)_2$-bpy}(mnt)] (**3c**) shows both reductions at the least negative potential of the series **1c** – **3c**, as expected,[12] however the first reduction potential (E_1) of [Pt{3,3′-$(CO_2Et)_2$-bpy}(mnt)] (**1c**) occurs at less negative potential than that of [Pt{4,4′-$(CO_2Et)_2$-bpy}(mnt)] (**2c**) which is in contrast with the reduction potentials of the free ligands **1a** and **2a**. The crystal structure of [Pt{3,3′-$(CO_2Et)_2$-bpy}(mnt)] previously reported by us[6] shows a significant torsion angle (30.7º) between the two pyridine rings of the bpy moiety while [Pt(II)(bpy)(dithiolate)] complexes with substituents at the 4,4′ positions have much smaller torsion angles e.g. 0.68° for a di-Me substituted bpy,[13] and 12.69° for a di-tBu substituted bpy[14] (the biggest for any 4,4′-disubstituted bpy). This suggests that the structural differences between the 3,3′ and 4,4′ disubstituted molecules influence their relative electrochemical responses and this results in the first reduction of **1c** being

intermediate between that of **2c** and **3c**. For each of the molecules studied, the separation of the first and second reduction is between 0.36 V and 0.66 V. This is associated with the spin pairing energy of the two added electrons in the same orbital (*vide infra*) .

The electrochemistry of the carboxylic acid substituted complexes (**1d, 2d** and **3d**) shows broadly similar oxidation and reduction potentials to those of the ester-substituted complexes (**1c, 2c** and **3c**), suggesting that the more-soluble ester species used for convenience in the further studies below are good models for the acid derivatives used in DSSC.

Table 2. EPR data for $\mathbf{1b}^{1-}$ and $\mathbf{1c}^{1-}$ in 0.1 M $TBABF_4$ in DMF at 293 K. All hyperfine coupling constants given in G with 10^{-4} cm^{-1} in parenthesis. Δ = linewidth

	$\mathbf{1b}^{1-}$	$\mathbf{1c}^{1-}$	$\mathbf{2b}^{1-}$	$\mathbf{2c}^{1-}$	$\mathbf{3b}^{1-}$	$\mathbf{3c}^{1-}$
a_{iso} (H×2)	3.7 (3.4)	4.0 (3.7)				
a_{iso} (N×2)	3.7 (3.4)	4.0 (3.7)				
a_{iso} (Pt)	45.5 (42.2)	42.0 (39.2)	59.5 (54.9)	56.0 (52.1)	39	36
Δ	4.1	4.3				
g	1.997	2.001	1.988	1.994	1.994	1.967

(ii) Spectroelectrochemistry

UV/Vis/NIR spectroelectrochemistry of reduced **1c**, **2c** and **3c** was reported in our prior work[6] and in this work we have also studied the spectroelectrochemistry of the corresponding species **1a,b**, **2a**,**b** and **3a**,**b** as well as oxidations of **1c**, **2c** and **3c**, which were observed to be chemically reversible at -60°C (observed absorptions are tabulated in supplementary information, Table S1, Fig S1-S4). Electrochemical reduction to the monoanionic and dianionic species for **1a-c**, **2a-c** and **3a-c** show similar trends. For the complexes **1-3b** and **1-3c**, similar bands appeared compared with the free ligands **1-3a** consistent with the reduction electron locating on the bpy ligand. Spectral features of the reduced, substituted bpy ligands in turn were similar to the unsubstituted bpy^{1-}.[15] Upon oxidation of **1c**, **2c** and **3c,** each of the spectra show similar features (e.g. Fig. S4). On generation of the $\mathbf{1c}^{1+}$, $\mathbf{2c}^{1+}$ and $\mathbf{3c}^{1+}$, the peaks associated with the π-π^* transition of the coordinated bpy shift to lower energy. This has previously been shown in a study of $[Ru(bpy)_3]^{3+}$ and $[Ir(bpy)_3]^{3+}$ where the π-π^* transition of the coordinated bpy shifted to lower energy as the positive charge on the complex was increased.[16,17] In the monooxidised species, the decrease in intensity of the peak at 19,000 cm^{-1}, which has already been assigned as a MMLL′CT peak from the mnt moiety, is consistent with the site of oxidation as based at least in part on the mnt motif.

(iii) EPR in fluid solution

In-situ EPR spectroelectrochemistry was performed on each member of the [Pt{X,X′-$(CO_2Et)_2$-bpy}(mnt)] series (**1c**, **2c**, **3c)** and comparison made where possible with the precursor species **1a,b**, **2a**,**b** and **3a,b**. Data observed were broadly comparable to previous studies of related complexes.[18]

(a) Reduced 3,3′-$(CO_2Et)_2$-bpy ligand and complexes ($\mathbf{1a^{1-}}$, $\mathbf{1b^{1-}}$, $\mathbf{1c^{1-}}$)

Reduction of **1c** in solution of 0.1 M $TBABF_4$ in DMF at 233 K gives an EPR active solution of $\mathbf{1c^{1-}}$. The coupling to the ligand nuclei is best resolved at 293 K (Fig. 3) and the coupling constants for $\mathbf{1c^{1-}}$ are presented, alongside those of $\mathbf{1b^{1-}}$ (Fig. S5) in table 2. Coupling is observed to the Pt centre, two ring N atoms and two ring H atoms. These are most likely to be the hydrogens in the 5,5′ positions as this has previously been shown to be the most electronically important position.[12] This assignment is supported by DFT calculations (*vide infra*) that show the LUMO of the neutral complex to have a much higher contribution from the ring carbons in the 5-position than any of the other carbon atoms of the ring (Table S4). On introduction of another electron to each complex and formation of $\mathbf{1b^{2-}}$ and $\mathbf{1c^{2-}}$ respectively, the signal collapses as the second electron enters the same orbital as the first and they spin pair. The similarities between the spectra of $\mathbf{1b^{1-}}$ and $\mathbf{1c^{1-}}$ are consistent with the reduction electron entering an orbital primarily located on the derivatised bpy motif analogous to the results found in the UV/Vis/NIR spectroelectrochemistry experiments. We were unable to obtain the spectrum for $\mathbf{1a^{1-}}$ due to poor stability in the reduced form.

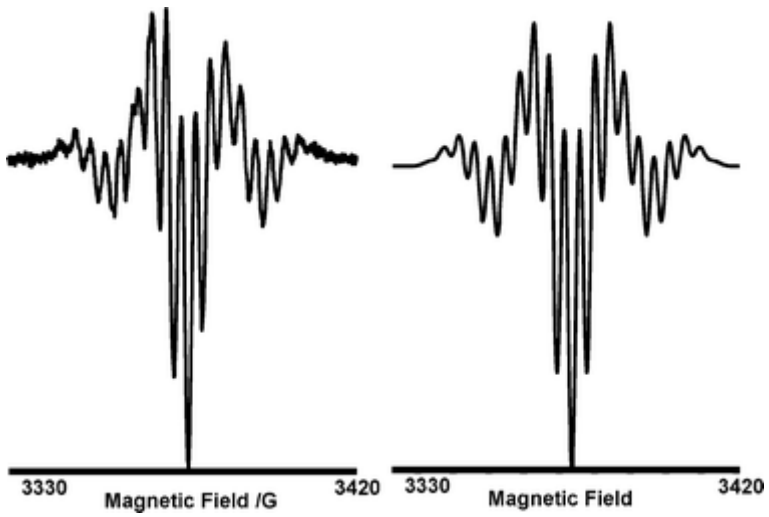

Figure 3. Left: 2nd derivative EPR spectrum of $\mathbf{1c^{1-}}$ in 0.1 M $TBABF_4$/DMF at 293 K. Right: simulated spectrum using parameters given in table 2.

Table 3. EPR coupling constants for **2a**$^{1-}$ and **3a**$^{1-}$ in 0.1 M $TBABF_4$/DMF at 233 K. All hyperfine coupling constants given in G. Δ = linewidth. For comparison, the calculated percentage contribution to the LUMO from the ring carbon and nitrogen atoms for the neutral compounds is given, with the position of the atom on the bipy ring shown in parenthesis.

Parameter	**2a**$^{1-}$	**%LUMO**	**3a**$^{1-}$	**%LUMO**
a_{iso}(H×2)	3.45	13.41 (5-position)	0.90	5.89 (4-position)
a_{iso}(H×2)	0.42	0.11 (6-position)	-	1.88 (6-position)
a_{iso}(H×2)	0.40	0.10 (3-position)	0.41	3.78 (3-position)
a_{iso}(N×2)	2.90	12.75	1.30	5.62
Δ	0.56		0.69	
g	2.004		2.003	

(b) Reduced 4,4′-$(CO_2Et)_2$-bpy ligand and complexes (2a^{1-}, 2b^{1-}, 2c^{1-})

In-situ reduction of the ligand (**2a**) gives an EPR active solution (Fig. 4) with coupling constants listed in table 3. The reduction electron couples strongly to the ring nitrogen and to one ring hydrogen on each pyridine ring. Again, the ring hydrogen atoms that show strong coupling can be assigned as those in the 5-position through DFT calculations that show the carbons in these positions to give much the largest contribution to the LUMO of the neutral compound compared with the other ring carbons (table 3).

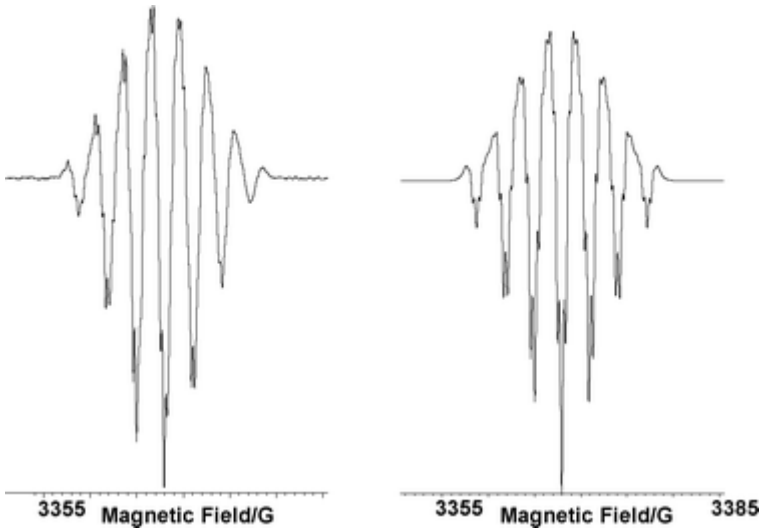

Figure 4. Left: EPR spectrum of **2a**$^{1-}$ in 0.1 M $TBABF_4$/DMF at 233 K. E_{gen} = -1.85 V. Right: simulated EPR spectrum of **2a**$^{1-}$ using parameters given in table 3.

The solution EPR of **2b**$^{1-}$ at 233K in solution of 0.1 M $TBABF_4$ in DMF shows a broad line with two ^{195}Pt satellites and any coupling to the ligand nuclei for this species remains unresolved at a range of temperatures. This is analogous to the *in-situ* EPR spectroelectrochemistry results for the related complex **2c**$^{1-}$. As was the case for **1b**$^{2-}$ and **1c**$^{2-}$, on introduction of another electron to form both **2b**$^{2-}$ and **2c**$^{2-}$ the signals collapse as the second electron enters the same orbital as the first and they spin pair forming a diamagnetic species.

(b) Reduced 5,5′-$(CO_2Et)_2$-bpy ligand and complexes (3a^{1-}, 3b^{1-}, 3c^{1-})

The *in-situ* EPR spectrum of the {5,5′-$(CO_2Et)_2$-bpy}$^{1-}$ ligand (**3a**$^{1-}$) shows coupling of the reduction electron to the two ring nitrogen atoms, and two sets of two ring hydrogen atoms assigned as shown in table 3. It is of note in this case that no large coupling to ring hydrogens occurs since the most electronically important 5-positions contain the ester substituents rather than H-atoms.

The solution EPR of **3b**$^{1-}$ at 273 K in solution of 0.1 M $TBABF_4$ in DMF shows coupling of the reduction electron to the ^{195}Pt nucleus. Any coupling to the ligand nuclei for this species remains unresolved at a range of temperatures similar to the results found for **2b**$^{1-}$. Again in this case the EPR spectrum of **3c**$^{1-}$ is analogous to the *in-situ* EPR spectrum for the related dichloride complex **3b**$^{1-}$ which shows a similar magnitude of the coupling of the reduction electron to the Pt nucleus.

Table 4. EPR parameters of compounds in 0.1 M $TBABF_4$/DMF at 173 K. The A_{iso} values are taken from solution the spectra. Nominal A_3 values of 20 G were used in the simulations as these are not resolved. The A_3 values in the table are calculated as $3A_{iso} - (A_1 + A_2)$. W_{1-3} refer to linewidths.

Compound	g_{iso}	g_1	g_2	g_3	A_{iso}/cm^{-1}	A_1 / cm^{-1}	A_2 / cm^{-1}	A_3 / cm^{-1}	W_1/ G	W_2/ G	W_3/ G
1b	1.9975	2.038	2.012	1.972	42.2x10^{-4}	44×10^{-4}	60×10^{-4}	23×10^{-4}	5	7	18
1c	2.0014	2.033	2.019	1.975	39.2x10^{-4}	40×10^{-4}	49×10^{-4}	29×10^{-4}	5	7	18
2c	1.994	2.044	2.025	1.936	52.1x10^{-4}	55×10^{-4}	64×10^{-4}	37×10^{-4}	8	8	20

(iv) EPR in frozen solutions

On cooling to 173 K rhombic X-band EPR spectra were obtained for **1b**$^{1-}$, **1c**$^{1-}$ and **2c**$^{1-}$ and, following spectral simulation, the parameters obtained are listed in table 4. For all compounds, the average of $g_1 + g_2 + g_3$ is in good agreement with $g_{iso.}$ The small shift in g_{iso} from the free electron value, g_e of 2.0023 suggests that there is only a small admixture of metal orbitals in the SOMO and that the reduction electron is therefore based

mainly on the bpy ligand. These results reiterate the findings of the UV/Vis/NIR spectroelectrochemical study whereby the reduction electron locates itself on the bpy motif. In each case, coupling was resolved to the ^{195}Pt nucleus for each of the g-components but no further splittings to ligand nuclei were resolved. Experimental and simulated spectra are shown in Figs. 5, 6 and S7. Previous studies have shown that the singly-occupied orbital in related complexes is of b_2 symmetry assuming C_{2v} point symmetry with metal contributions to the singly occupied orbital consisting of $5d_{yz}$ and $6p_z$ contributions. (The principle axes are defined as shown in Fig. 1.[18]) The contribution of these orbitals to the SOMO can be determined using equations (1) – (3).[18,19]

$$A_{xx} = A_s - (4/7)P_d a^2 - (2/5)P_p b^2 \quad (1)$$

$$A_{yy} = A_s + (2/7)P_d a^2 - (2/5)P_p b^2 \quad (2)$$

$$A_{zz} = A_s + (2/7)P_d a^2 + (4/5)P_p b^2 \quad (3)$$

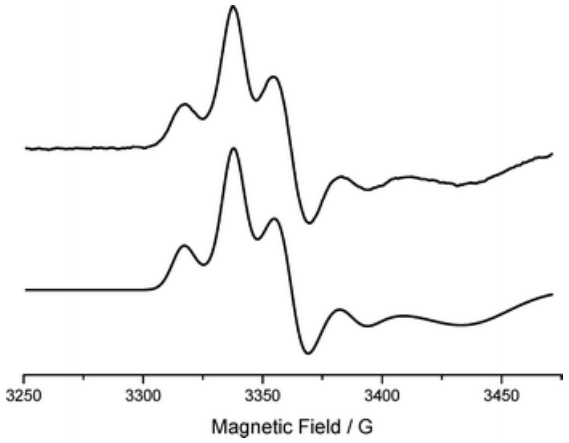

Figure 5. EPR spectrum of **1c**$^{1-}$ in solution of 0.1 M $TBABF_4$ in DMF at 173 K. E_{gen} = - 2.0 V. Simulated spectrum shown beneath.

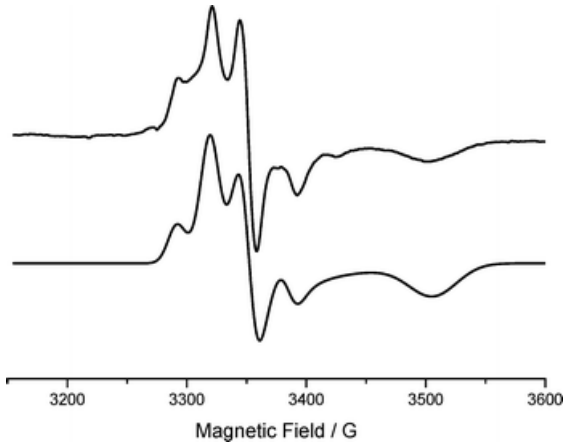

Figure 6. EPR spectrum of **2c**$^{1-}$ in solution of 0.1 M $TBABF_4$ in DMF at 173 K. E_{gen} = -1.15 V. Simulated spectrum shown beneath.

The parameters a^2 and b^2 are respectively the contribution of $5d_{yz}$ and $6p_z$ to the SOMO, P_d and P_p are the electron nuclear dipolar coupling parameters for platinum 5d and 6p electrons respectively and A_s is the isotropic Fermi contact term. Using calculated values $P_d = 0.0549$ cm^{-1} and $P_p = 0.0402$ cm^{-1},[20] we can derive values for a^2 and b^2 (table 5).

Table 5. Platinum $5d_{yz}$ and $6p_z$ admixtures and total contribution to the SOMO of the anions determined by EPR, compared with hybrid-DFT calculations of the Pt contribution to the LUMO and to the HOMO of the neutral complexes.

	a^2	b^2	Total Pt SOMO (EPR)		Total Pt LUMO (calc.)	Total Pt HOMO (calc.)
1b^{1-}	0.034	0.050	0.084	**1b**	0.078	0.429
1c^{1-}	0.019	0.023	0.042	**1c**	0.058	0.118
2c^{1-}	0.019	0.073	0.092	**2c**	0.083	0.106
				3c		0.111

This allows us to compare the effects of mnt substitution for two chloride ligands by examination of the values for **1b**$^{1-}$ and **1c**$^{1-}$. It is apparent that a reduction in Pt contribution to the SOMO occurs in the mnt complex **1c**$^{1-}$ and this may be associated with greater electron delocalisation in the latter consistent with the extended conjugation of the mnt. Likewise, we can compare the influence of altering the ester groups from the 4,4' to the 3,3'-positions (**2c**$^{1-}$ and **1c**$^{1-}$). The former shows a noticably higher Pt contribution to the SOMO. This may be rationalised in terms of a better overlap between the bpy and the Pt orbitals for the 4,4'-derivative due to greater planarity across the molecules, whereas the twist in the bpy ligand of the 3,3'-analogue reduces the orbital overlap of the bpy ligand with the Pt centre.

(v) DFT Calculations and Discussion

To further interpret the electronic character of these complexes, hybrid Density Functional Theory (DFT) calculations were performed on **1b**, **1c**, **2a**, **2c**, **3a** and **3c** (see experimental section for details). Plots of the isosurfaces and calculated energies of the HOMO, LUMO, HOMO-1 and LUMO+1 orbitals can be found in Fig 7 (**1c**) and in the supplementary information (Fig. S8 – S17). A comparison of selected angles and bond distances from the calculated structure of **1c** and the XRD structure shows that the calculated structure is very close to that experimentally observed, Table S6. All calculations are consistent with the HOMO based largely on the mnt moiety and the LUMO largely based on the bpy moiety (Table S7) as previously reported, with a larger total contribution of Pt orbitals to the HOMO than to the LUMO (table 5) for **1c**, **2c** and **3c**.[1,2,10] For the dichloride **1b**, the Pt contribution to the HOMO is seen to be much larger than for the three mnt-complexes in

keeping with the capacity of the dithiolene ligand to enhance delocalisation of the frontier orbitals in the complex. We also observe that the Pt contribution to the LUMO in **1b**, **1c** and **2c** matches the trend for the Pt contribution to the SOMO determined from the EPR results. In fact, there is also a reasonable match with the absolute values however, although gratifying, this may be fortuitous and it is the reproduction of the trend that is most significant.

The noticable difference in the Pt contribution to the LUMO/SOMO of **1c**/**1c**$^{1-}$ compared with **2c**/**2c**$^{1-}$ is likely to be due to the non-planar character of the former caused by the steric hindrance at the 3,3'-positions and we can therefore surmise that this causes poorer overlap with the Pt orbitals. Furthermore, the computational results show clear evidence of the consequences of this non planarity in the LUMO and LUMO+1 orbitals (Fig. 7). In particular, the latter orbital is localised on one of the pyridyl rings of the ligand only in complete contrast to the corresponding orbital for the planar **2c** (Fig. S13) which is distributed over the whole bpy ligand.

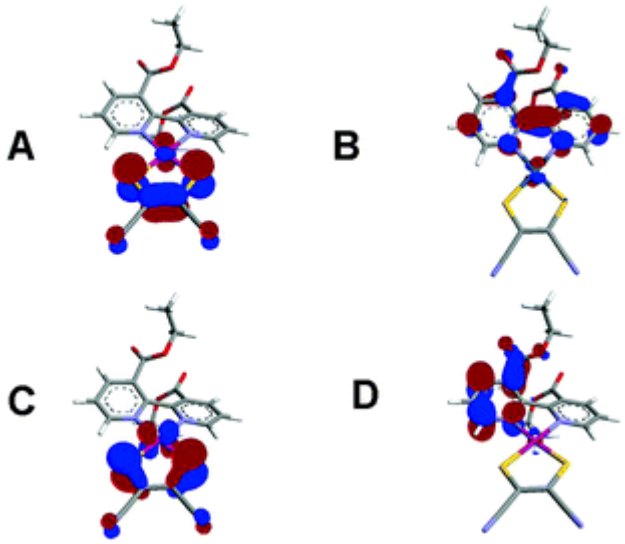

Figure 7. **A.** Calculated HOMO of **1c**. **B.** Calculated LUMO of **1c. C.** Calculated HOMO-1 of **1c. D.** Calculated LUMO+1 of **1c**

TD-DFT calculations were carried out for **1c**, **2c** and **3c** in the presence of DMF. This method has been previously used on similar platinum-diimine-dithiolate systems to great effect with the results showing a remarkable similarity to experimental observations.[21,22] A summary of relevant calculated transitions for each complex can be found in Tables S8-10 and figures showing the calculated transitions relative to the observed absorption spectrum are shown in Figures 8 and S18. The calculated composition of the lowest energy transition for all three complexes was found to be 70 % HOMO-LUMO and MMLL'CT in nature as expected.

The calculated energy was slightly underestimated, by an average of 1660 cm^{-1}, for all three complexes. It should be noted that the inclusion of solvent in these calculations is essential, as has been observed previously in similar systems,[23] as the TD-DFT studies carried out in vacuum vastly underestimated the energy of the MMLL'CT by ~ 12000 cm^{-1}. The highest energy transitions were identified as bpy intraligand transitions and calculated to be no more than 900 cm^{-1} from those observed. The relative size of the oscillator strengths match the relative intensities of the observed spectra well, with the bpy intraligand transitions being the most intense and the two CT bands being of a similar magnitude to one another. Lastly, the observed trend in the energy of the HOMO-LUMO transitions was reproduced with **1c** being the lowest and **2c** being the highest.

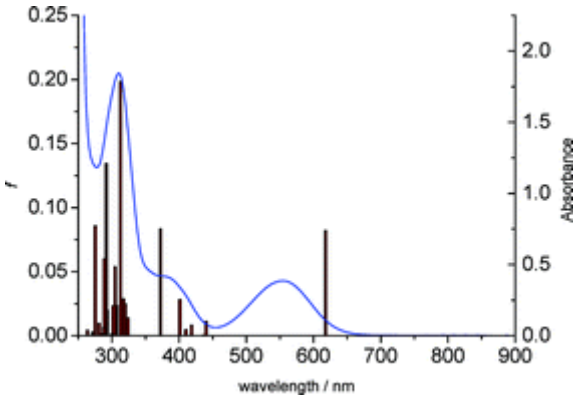

Figure 8. Calculated TD-DFT results shown as bar chart (left axis) relative to the observed absorption spectrum (right axis) in DMF of **1c**.

In our prior work we determined that **1c** showed a better solar-to-electric power-conversion efficiency than **2c** (and much better that **3c**).[6] In particular this arose from a higher open-circuit voltage for a cell using **1c** which was explained by the longer charge recombination time (between electrons in the TiO_2 and the oxidised dye) that was determined for this complex.[6] This charge-recombination is known as a key loss process and its inhibition is one of the widely-studied approaches to dye design for DSSC.[24]

The results presented in this work suggest that the longer-lived charge-separated state for complex **1c** on TiO_2 is related to the non-planar geometry of the complex. We have shown, by the lower contribution of the Pt orbitals to the SOMO/LUMO of **1c** compared with **2c** as shown by EPR/DFT studies, that this reduces the electronic coupling between the bpy ligand and the Ptmnt fragment of the dye as well as reducing the electronic coupling across the bpy ligand itself. According to the electrochemical and spectroelectrochemical results, the positive charge density on the oxidised dye is located largely on the mnt ligand and this conclusion is supported by DFT calculation of the HOMO location on the neutral complexes. The poorer electron

delocalisation across the dye in the case of **1c** will then lead to poorer electronic communication between the cation on the dye and electrons in the TiO_2 giving a longer-lived charge-separated state.

Interestingly, the observation of significantly poorer photovoltaic performance using **3c** is also consistent with this analysis. The electrochemical and EPR results in this work and previous ENDOR results demonstrate that the 5,5′-positions on the bpy are the most strongly electronically coupled to the ring. Thus, the poor performance of **3c** may in part be explained by enhanced charge recombination via strong electronic communication from the TiO_2 to the positive charge on the oxidised dye via the acids group in the 5-position of the bpy.

Conclusions

This work contains the first detailed spectroelectrochemical (UV/Vis/NIR and EPR) and DFT study on a family of [Pt(diimine)(dithiolate)] dyes and their synthetic precursors. These molecules are important in their relevance to the area of solar cell dyes and also more generally for their optical and electronic functionality. The OTTLE and *in-situ* EPR experiments confirm previous investigations which assign the location of the bpy based LUMO, although they also demonstrate partial involvement of the metal centre in the LUMO as indicated by coupling of the reduction electron to the Pt nucleus, supported by computational results. Trends in the OTTLE study of the mnt dyes indicate that in general the location of the reduction electron is similar within the 3,3′, 4,4′ and 5,5′ motifs.

Most significantly, the EPR and DFT studies provide a rationale for the superior performance of the 3,3'-substituted bpy-complex over the 4,4'-substituted bpy counterpart in DSSC. This provides important guidance in the optimisation of such solar cell dyes in future studies and we suggest that the focus in the DSSC field on 4,4′-bipy ligands with almost no investigation of 3,3′-bipy may be a missed opportunity for dye enhancement.

Experimental

The synthesis of each compound **1**-**3**(**a**-**d**) has previously been reported.[6] Electrochemical studies were carried out using a DELL GX110 PC with General Purpose Electrochemical System (GPES), version 4.8, software connected to an autolab system containing a PGSTAT 20 potentiostat. The technique used a three electrode configuration, with a 0.5 mm diameter Pt disc working electrode, a Pt rod counter electrode and an Ag/AgCl (saturated KCl) reference electrode against which the ferrocenium/ferrocene couple was measured to be +0.55 V. The supporting electrolyte was 0.1 M tetrabutylammonium tetrafluoroborate ($TBABF_4$), solvent was dry, degassed DMF and concentration of compound approximately 1 mmol.

OTTLE (Optically Transparent Thin Layer Electrode) measurements were taken using a quartz cell of 0.5 mm, a Pt/Rh gauze working electrode, an Ag/AgCl reference electrode and a Pt wire counter electrode. UV-vis spectra were recorded on a Perkin-Elmer Lambda 9 spectrophotometer, controlled by a Datalink PC, running UV/Winlab software. 0.1 M $TBABF_4$ was used as the supporting electrolyte in all cases.[25]

All *in-situ* EPR spectra were recorded on an X-band Bruker ER200D-SCR spectrometer, connected to datalink 486DX PC running EPR Acquisition System, version 2.42 software. *In-situ* EPR experiments were electrogenerated using a BAS CV-27 voltammograph. Variable temperature work was carried out using a Bruker ER111VT variable temperature unit. In some cases, solution spectra were recorded at reduced temperature to ensure long-term stability of the reduced species. All g values were corrected to 2,2'-diphenyl-1-picrylhydrazyl with $g_{literatue} = 2.0036 \pm 0.0002$. Spectra were simulated by manipulation of parameters until a satisfactory reproduction of experimental spectra was obtained, assuming couplings to the following nuclei: ^{195}Pt (I = ½, 33.8% abundance), ^{1}H (I = ½, 100% abundance) and ^{14}N (I = 1, 100% abundance). Since each of these gives a different combination of nuclear spin (hence splitting) and natural abundance, no ambiguity in nuclear types arises in the simulations.

Density functional theory calculations of all complexes were performed using either the Gaussian 03 program package[26] or the GAMESS-UK package.[27] The starting structure was input using the builder program Arguslab and default convergence conditions of Gaussian 03 were used. The Becke three parameters hybrid exchange and the Perdew-Wang 1991 correlation functionals (B3PW91) were used.[28, 29] For the platinum atom the Hay-Wadt VDZ (n+1) ECP was used[30] with the other atoms described by 6-31G*.[31] The optimised structures were verified as minima on the potential energy surface by the absence of negative values in the frequency calculations. TD-DFT calculations were carried out in the presence of a polarisable continuum model (PCM) DMF[32] solvation field, with the first 25 singlet transitions calculated.

References

[1] S. D. Cummings and R. Eisenberg, *J. Am. Chem. Soc.*, 1996, **118**, 1949.

[2] M. Hissler, J. E. McGarrah, W. B. Connick, D. K. Geiger, S. D. Cummings, and R. Eisenberg, *Coord. Chem. Rev.*, 2000, **208**, 115.

[3] E. A. M. Geary, N. Hirata, J. Clifford, J. R. Durrant, S. Parsons, A. Dawson, L. J. Yellowlees, and N. Robertson, *Dalton Trans.*, 2003, 3757.

[4] A. Islam, H. Sugihara, K. Hara, L. Pratap Singh, R. Katoh, M. Yanagida, Y. Takahashi, S. Murata, and H. Arakawa, *New J. Chem.*, 2000, **24**, 343.

[5] A. Islam, H. Sugihara, K. Hara, L. P. Singh, R. Katoh, M. Yanagida, Y. Takahashi, S. Murata, H. Arakawa, and G. Fujihashi, *Inorg. Chem.*, 2001, **40**, 5371.

[6] E. A. M. Geary, L. J. Yellowlees, L. A. Jack, I. D. H. Oswald, S. Parsons, N. Hirata, J. R. Durrant, and N. Robertson, *Inorg. Chem.*, 2005, **44**, 242.

[7] J. Zhang, P. Du, J. Schneider, P. Jarosz, R. Eisenberg, *J. Am. Chem. Soc.,* 2007, **129**, 7726

[8] M. K. Nazeeruddin and M. Graetzel, *Comp. Coord. Chem. II*, 2004, **9**, 719.

[9] E. Galoppini, *Coord. Chem. Rev.*, 2004, **248**, 1283; N. Robertson, *Angew. Chem.Int. Ed.,* 2006, **45**, 2338

[10] W. Paw, S. D. Cummings, M. A. Mansour, W. B. Connick, D. K. Geiger, and R. Eisenberg, *Coord. Chem. Rev.*, 1998, **171**, 125.

[11] P-H. Xie, Y-J Hou, T-X Wei, B-W. Zhang, Y. Cao, C-H. Huang, *Inorg. Chim. Acta,* 2000, **308**, 73; Y-J. Hou, P-H. Xie, B-W. Zhang, Y. Cao, X-R. Xiao, W-B. Wang, *Inorg. Chem.,* 1999, **38**, 6320

[12] L. Jack, Ph.D. Thesis, University of Edinburgh, 2003.

[13] J. M. Bevilacqua and R. Eisenberg, *Inorg. Chem.*, 1994, **33**, 2913.

[14] B. W. Smucker, J. M. Hudson, M. A. Omary, and K. R. Dunbar, *Inorg. Chem.*, 2003, **42**, 4714.

[15] E. Koenig and S. Kremer, *Chem. Phys. Lett.*, 1970, **5**, 87.

[16] V. T. Coombe, G. A. Heath, A. J. MacKenzie, and L. J. Yellowlees, *Inorg. Chem.*, 1984, **23**, 3423.

[17] G. A. Heath, L. J. Yellowlees, and P. S. Braterman, *Chem. Commun.*, 1981, 287.

[18] E. J. L. McInnes, R. D. Farley, C. C. Rowlands, A. J. Welch, L. Rovatti, L. J. Yellowlees, *J. Chem. Soc. Dalton Trans.,* **1999**, 4203

[19] P. H. Rieger, *J. Magn. Reson.,* 1997, **124**, 140

[20] E. J. L. McInnes, R. D. Farley, S. A. MacGregor, K. J. Taylor, L. J. Yellowlees, C. C. Rowlands, *J. Chem. Soc. Faraday Trans.,* **1998**, 2985

[21] C. J. Adams, N. Fey, M. Parfitt, S. J. A. Pope and J. A. Weinstein, *Dalton Trans.*, 2007, 4446-4456.

[22] C. Makedonas and C. A. Mitsopoulou, *Eur. J. Inorg. Chem.*, 2006, 2460-2468; C. Makedonas, C. A. Mitsopoulou, F. J. Lahoz, A. I. Balana, *Inorg. Chem.,* 2003, **42**, 8853

[23] A. Vlček Jr., S. Záliš, *Coord. Chem. Rev.,* 2007, **251***,* 258-287.

[24] N. Hirata, J-J Lagref, E. J. Palomares, J. R. Durrant, M. K. Nazeeruddin, M. Grätzel, D. Di Censo, *Chem. Eur. J.,* 2004, **10**, 595

[25] E. Alessio, S. Daff, M. Elliot, E. Iengo, L. A. Jack, K. G. Macnamara, J. M. Pratt, L. J. Yellowlees, Spectroelectrochemical techniques. Trends in Molecular Electrochemistry **2004**, 339

[26] Gaussian 03, Revision C.02, M. J. Frisch, G. W. Trucks, H. B. Schlegel, G. E. Scuseria, M. A. Robb, J. R. Cheeseman, J. A. Montgomery, Jr., T. Vreven, K. N. Kudin, J. C. Burant, J. M. Millam, S. S. Iyengar, J. Tomasi, V. Barone, B. Mennucci, M. Cossi, G. Scalmani, N. Rega, G. A. Petersson, H. Nakatsuji, M. Hada, M. Ehara, K. Toyota, R. Fukuda, J. Hasegawa, M. Ishida, T. Nakajima, Y. Honda, O. Kitao, H. Nakai, M. Klene, X. Li, J. E. Knox, H. P. Hratchian, J. B. Cross, V. Bakken, C. Adamo, J. Jaramillo, R. Gomperts, R. E. Stratmann, O. Yazyev, A. J. Austin, R. Cammi, C. Pomelli, J. W. Ochterski, P. Y. Ayala, K. Morokuma, G. A. Voth, P. Salvador, J. J. Dannenberg, V. G. Zakrzewski, S. Dapprich, A. D. Daniels, M. C. Strain, O. Farkas, D. K. Malick, A. D. Rabuck, K. Raghavachari, J. B. Foresman, J. V. Ortiz, Q. Cui, A. G. Baboul, S. Clifford, J. Cioslowski, B. B. Stefanov, G. Liu, A. Liashenko, P. Piskorz, I. Komaromi, R. L. Martin, D. J. Fox, T. Keith, M. A. Al-Laham, C. Y. Peng, A. Nanayakkara, M. Challacombe, P. M. W. Gill, B. Johnson, W. Chen, M. W. Wong, C. Gonzalez, and J. A. Pople, Gaussian, Inc., Wallingford CT, 2004.

[27] GAMESS-UK is a package of ab initio programs. See: "http://www.cfs.dl.ac.uk/gamess-uk/index.shtml", M.F. Guest, I. J. Bush, H.J.J. van Dam, P. Sherwood, J.M.H. Thomas, J.H. van Lenthe, R.W.A Havenith, J. Kendrick, "The GAMESS-UK electronic structure package: algorithms, developments and applications", Molecular Physics, Vol. 103, No. 6-8, 20 March-20 April 2005, 719-747.

[28] J.P.Perdew, J.A. Chevary, S.H. Vosko, K.A. Jackson, M.R. Pederson, D.J. Singh and C.Fiolhais, *Phys Rev. B*, 1993, **48**

[29] J.P. Perdew, K. Burke and Y. Wang, *Phys. Rev. B*, 1996, **54**, 16533.

[30] P.J. Hay, W.R. Wadt, *J. Chem. Phys*, 1985, **82**, 299.

[31] M. M. Francl, W. J. Pietro, W. J. Hehre, J. S. Binkley, M. S. Gordon, D. J. Defrees and J. A. Pople, *J. Chem. Phys.*, 1982, **77**, 3654.

[32] E. S. Boes, P. R. Livotto, H. Stassen, *Chem. Phys.*, 2006, **331**, 142.